TEMPO-oxidized Nanofibrillated Cellulose Film (NFC) incorporating Graphene Oxide (GO) Nanofillers

Yoojin Kim

Thesis submitted to the faculty of the Virginia Polytechnic Institute and State University in partial fulfillment of the requirements for the degree of

Master of Science
In
Macromolecular Science and Engineering

Young Teck Kim
Kevin Edgar
Maren Roman

December 15, 2017
Blacksburg, Virginia

Keywords: nanofibrillated cellulose, TEMPO, graphene oxide, nanocomposite, homogenization

TEMPO-oxidized Nanofibrillated Cellulose Film (NFC) incorporating Graphene Oxide (GO) Nanofillers

Yoojin Kim

ABSTRACT

The development of a new class of alternative plastics has been encouraged in the past few years due to the serious environmental issues, such as toxicity and carbon dioxide emissions. Hence, the introduction of renewable, biodegradable, and biocompatible materials is becoming critical as substituents of conventional synthetic plastics. To design a new system of novel TEMPO-oxidized cellulose nanofibrils (TOCNs)/graphene oxide (GO) composite, the 2,2,6,6-tetramethylpiperidine-1-oxyl radical (TEMPO)-mediated oxidation was utilized to disintegrate never-dried wood nanofibrillated cellulose (NFC). GO was incorporated through high intensity homogenization and ultrasonication with varying degree of oxidation (0.5X, 1X, and 2X) of NFC and GO percent loadings: 0.4, 1.2, and 2.0wt %. As a result, despite the presence of carboxylate groups and graphene oxide (GO), X-ray diffraction (XRD) test showed the crystallinity of the bio-nanocomposite was not altered. Scanning electron microscopy (SEM) was used to characterize their morphologies. In addition, the thermal stability of TOCN/GO composite decreased upon oxidation level, and dynamic mechanical analysis (DMA) signified strong intermolecular interactions with the improvement in Young's storage modulus, and tensile strength. Fourier transform infrared spectroscopy (FTIR) was employed to see the hydrogen bonds between GO and cellulosic polymer matrix. The oxygen transmission rate (OTR) of TOCN/GO composite decreased. The water vapor permeability (WVP) was not significantly affected by the reinforcement with GO, but the moderate oxidation enhanced the barrier properties. Ultimately, the newly fabricated TOCN/GO composite can be utilized in a wide range of life science applications, such as food and medical industries.

GENERAL AUDIENCE ABSTRACT

In recent years, petroleum-based polyolefins have been contributing to severe environmental issues. With this in perspective, the development of a new class of alternative plastics has been encouraged. Hence, the introduction of renewable, biodegradable, and biocompatible materials is becoming critical as a substitute for non-degradable synthetic plastics. In this study, a new system of novel cellulose-based plastic composites was designed by incorporating carbon nanofillers at various percent loadings and different degree of surface modification of the plastics. These treatments are the economical way to achieve the targeted properties for industrial applications, exhibiting the obvious improvement in tensile strength due to the strong interaction between nanofillers and cellulose. In addition, water vapor and oxygen barrier properties play significant roles in food packaging since food decay is vulnerable to these two factors. The barrier performance was enhanced by hindering the permeation of oxygen gases, whereas the water vapor permeability was not significantly affected by the reinforcement with carbon nanofillers. Ultimately, the newly fabricated cellulose plastic can be utilized in various applications, especially, such as the pharmaceutical and biomedical area, packaging for food and goods, and agriculture due to their high availability, sustainability, and biodegradability.

TABLE OF CONTENTS

3.4. Characterization

3.5. Results and Discussion

CHAPTER 1. INTRODUCTION

A material composed of two or more components, showing different chemical or physical properties, is termed a "composite." Composites after their intended life go to either landfills or incineration plants since they are hard to separate into the original components and recycle.[1]In recent years, petroleum-based polyolefins have been contributing to severe environmental issues. Petroleum-based nonreplenishable plastics do not degrade under enzymatic conditions by microorganisms over a long period of time.[1]Unfortunately, the landfill area available for the disposal of wastes has drastically decreased. For instance, the number of landfills in the United States has fallen from 8000 to 2314 since 1988.[2] Based on the estimated consumption rate of petroleum, the rate of depletion is 100,000 times more rapid than the rate of extraction in nature. Environmental issues, such as toxicity and carbon dioxide emissions, also bring about serious negative consequences. The amount of conventional plastics produced globally has nearly reached 200 million tons per year, whereas the amount of bioplastics produced is limited to approximately 750,000 tons per year.[3]Therefore, the development of a new class of alternative plastics has been encouraged in the past few years.

The introduction of renewable, biodegradable, and biocompatible materials is becoming critical as substitutes for conventional synthetic plastics. For example, aliphatic polyesters, such as poly(lactic acid) (PLA), poly(butylenesuccinate) (PBS), poly(hydroxybutyrate-co-valerate) (PHBV), and polycaprolactone (PCL), have emerged in many studies due to their high biodegradability.[4] Besides the biodegradable polymers above, cellulose materials – wood flour and wheat straw– are also newly considered as valuable alternatives to traditional plastics in order to make cellulosic plastics.[5] Natural fibers are also believed to be eco-efficient and environment-friendly bio-based materials.[1] They are regarded as worthwhile due to their low

cost, high availability, sustainability, biocompatibility, and biodegradability.[6] Unlike petroleum-based materials, biodegradable plastics can be degraded by the enzymatic activities of microorganisms or bacteria after their intended lives without ecotoxic effects, showing higher degradation rates.[1, 3] The life cycle of biodegradable plastics is shown in Figure 1. As a result, natural fibers have been used in a variety of areas, such as the pharmaceutical and biomedical area, packaging for food and goods, and agriculture due to the commercial viability and environmental acceptability.[3]

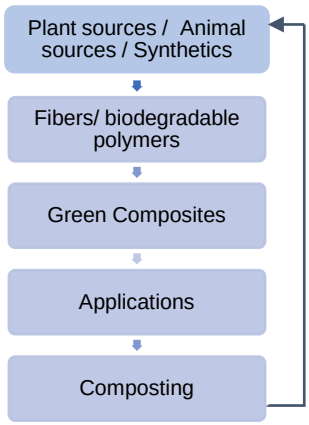

Figure 1. Life cycle of biodegradable plastics[1]

Nevertheless, the use of the biodegradable plastic itself is limited since the poor thermal and mechanical properties of pristine biomaterials are not sufficient for long-term use. Therefore, designing a new system of novel composites is a practical solution of addressing the drawbacks and enhancing the properties of the final products.[5] A variety of nanofillers, such as organoclay, carbon nanotubes(CNT), graphene oxide (GO), polysilsesquioxane, and silica, have been incorporated in polymer matrices through solution mixing, in situ polymerization or melt-based mixing methods to fabricate value-added bio-composites.[5]

REFERENCES

1. Netravali, A. N.; Chabba, S., Composites get greener. *Materials today* **2003,***6* (4), 22-29.
2. Stevens, E. S., *Green plastics: an introduction to the new science of biodegradable plastics*. Princeton University Press: 2002.
3. Gironi, F.; Piemonte, V., Bioplastics and Petroleum-based Plastics: Strengths and Weaknesses. *Energy Sources, Part A: Recovery, Utilization, and Environmental Effects* **2011,***33* (21), 1949-1959.
4. Wang, J.; Zheng, L.; Li, C.; Zhu, W.; Zhang, D.; Xiao, Y.; Guan, G., Fully biodegradable blends of poly (butylene succinate) and poly (butylene carbonate): Miscibility, thermal properties, crystallization behavior and mechanical properties. *Polymer Testing* **2012,***31* (1), 39-45.
5. Wan, C.; Chen, B., Reinforcement of biodegradable poly (butylene succinate) with low loadings of graphene oxide. *Journal of Applied Polymer Science* **2013,***127* (6), 5094-5099.
6. Wei, H.; Rodriguez, K.; Renneckar, S.; Vikesland, P. J., Environmental science and engineering applications of nanocellulose-based nanocomposites. *Environmental Science: Nano* **2014,***1* (4), 302-316.

CHAPTER 2. REVIEW OF LITERATURE

2.1. Chemical Structure of Cellulose

Cellulose has received attention due to its high availability and sustainability. In general, cellulose which exists in plant cell walls of wood or cotton is highly abundant biopolymer, and nature produces approximately 10^6 tons annually.[1-2] Natural fibers are mainly composed of cellulose, hemicellulose, and lignin. The structure constitutes of a soft matrix of hemicellulose and lignin and the embedded cellulose fibrils.[3-4] According to the different origins of the plants, chemical composition, cell dimension, the inside of the fiber structure, and defects are appreciably different, and these factors affect the ultimate properties of cellulose.[5]Two major polymorphs of cellulose exist: cellulose I and cellulose II. Cellulose I, known as native cellulose, represents the crystalline cellulose produced by the sources, such as trees, plants, bacteria, algae, and tunicates.[6] Native cellulose mostly exists in the combination of cellulose I_α and I_β.[7] Cellulose I_α, which has a triclinic crystal system, is prevalent in bacterial celluloses, whereas the monoclinic I_β form is dominantly in annual plants – cotton and ramie.[7]As an example of cellulose I, the cellulose tunicin, obtained from tunicate – a family of sea animals – is made up of about 90% of I_β form while freshwater alga *Glaucocystis sp.* is composed of approximately 90% of I_α form.[7] Thermodynamically metastable cellulose $I_\alpha$can be changed into I_β form via annealing.[7]Cellulose I has been widely used as a nanofiller because of its high modulus and crystallinity, which are attributed to good mechanical properties. The more stable cellulose II, called regenerated cellulose, indicates the precipitated cellulose from solutions, such as alkali solutions.[7]It shows a monoclinic form, which has been utilized for producing cellophane.[6]

Cellulose comprises a β-D-glucopyranose repeat unit, which is a six-membered ring including five carbon atoms and one oxygen atom. When an acetal is formed with the reaction between alcohol and hemiacetal in the ring, a water molecule is removed, leaving the repeating units of β-1,4-D-anhydroglucopyranose ($(C_6H_{10}O_5)_n$; n=10,000 to 15,000, dependent on the origin of the cellulose polymer);[6,8]C1 of a glucopyranose ring and C4 of the adjacent ring are hooked together by covalent bonds with an oxygen between them.[9] These bonds are called β-1,4linkages.[10]

Figure 1. The chemical structures of cellulose and starch

The benefit of the β configuration at the C1 atom, as shown in Figure 1, is that all the functional groups of β-glucose monomers are in equatorial positions, and this structure leads the cellulose polymer chains to have a linear configuration rather than a coil. It contributes to an excellent fiber-forming candidate.[11] Furthermore, hydrogen bonds play a decisive role in terms of the formation of a fibril, which is long thread-like molecular strands, from the chains of 1,4-β-D-glucosyl residues.[12-15] In other words, as presented in Figure 2, intermolecular interactions – van der Waals and hydrogen bonds between oxygens and hydroxyl groups (-OH) – result in the aggregation of fibrils, forming microfibril bundles.[6] Each fibril is linked together by multiple

intermolecular bonds, governing the crystalline packing and physical properties of cellulose,[7] that is to say the high axial chain stiffness.[17]

Figure 2. The schematic illustration of intermolecular and intramolecular hydrogen bonds within the cellulose[18]

Moreover, the reason that cellulose $I_\alpha$is regarded as thermodynamically metastable is also ascribed to hydrogen bonds within the fibrils. They are easily broken even at lower temperatures, the I_α polymorph has lower stability than I_β.[6]On the contrary, cellulose II is considered to be thermodynamically stable due to the interlayer hydrogen bonds on glucosyl residues that are absent in cellulose I. In general, the singular cellulose nanofibril is 2 to 20 nm in diameter and a few microns in length.[9, 19]Table 1 provides different types of cellulose particle characteristics.

Furthermore, the cellulose fibrils constitute mixtures of highly ordered crystalline and disordered amorphous structures.[6] Within the native celluloses, there are 65-95% of crystalline regions based on their source materials. Despite the effort to disintegrate microfibrils mechanically, it is impossible to obtain completely individualized cellulose fibrils due to a number of hydrogen bonds.[20] Therefore, it is suggested to achieve a further individualization of cellulose fibrils with several chemical and repeated treatments using a high-pressure homogenizer in a highly swollen state in water.[21-22]

Table 1. Summary of physical properties of several cellulose particles[6]

Particle Type	Length (μm)	Width (nm)	Height (nm)	Crystallinity (%)
WF/PF	>2000	20-50	20-50	43-65
MCC	10-50	10-50	10-50	80-85
MFC	0.5-10's	10-100	10-100	51-69
NFC	0.5-2	4-20	4-20	-
CNC	0.05-0.5	3-5	3-5	54-88
t-CNC	0.1-4	~20	~8	85-100
BC (Acetobacter)	>1	30-50	6-10	63

2.2. A Variety of Nanocellulose Materials Based on Different Disintegration Methods

Since the kraft pulps have matrix materials - hemicellulose and lignin - pretreatments to remove these materials are required to use the pure cellulose as a starting material for TEMPO-mediated oxidation.[6, 23] The mechanical pretreatment should also be applied to reduce the size of the cellulose fibers to prevent the cellulose suspension from clogging in the high pressure homogenizer.[24] Specifically, the raw materials are initially milled and passed through alkali and bleaching treatments. These treatments leave the cellulose components largely intact, while removinglignins and hemicelluloses.[7]In general, use of never-dried cellulose is preferred since hydrogen bonds between the fibrils promote aggregation upon drying.[6] Since most of the hydrogen bonds cannot be replaced even with rehydration of once-dried cellulose, the fibrils do not go back to their original state.[6]

The bleached fibers are then treated via surface modification, acid hydrolysis, or high intensity homogenization.[7] For surface modification, for example, TEMPO regioselective oxidation, sulfonation, acetylation, or grafting with an anionic polyelectrolyte have been widely used.[1, 6, 24]As mentioned before, nanocellulose can be found in a variety of forms as shown in Figure 3, depending on the source materials, the extraction processes, or chemical treatments. Those different cellulose types are designated by distinctive names – long and microfibrillated

cellulose (MFC) and nanofibrillated cellulose (NFC); cellulose whiskers, namely cellulose nanocrystal (CNC); andbacterial cellulose (BC).[25]For instance, bacterial cellulose (BC) is formed by particular bacterial strains from genus, such as *Achromobacter, Alcaligenes,* and *Gluconacetobacter.*[25] In Table 2, a summary of the mechanical properties of cellulose and some reinforcement materials is given.

Table 2. Mechanical properties of cellulose nanoparticles and neat films vs. comparative materials[6]

Material	E (GPa)	E_A (GPa)	σ_f(GPa)
Carbon fiber	—	150–500	1.5–5.5
Steel Wire	—	210	4.1
Carbon Nanotubes	—	270–950	11–63
Crystalline Cellulose	—	110–220	7.5–7.7
Kevlar-49 fiber	—	124–130	3.5
WF			
particles	—	14–27	0.3–1.4
film	4-9	—	0.045-0.08
PF (particle)	—	5–45	0.3–0.8
MCC (particle)	—	25 ± 4	—
MFC (film)	1–17.5	N/A	0.03–0.156
NFC (film)	6–15	—	0.095–0.24
CNC			
particle	—	57, 105	—
film	6		—
t-CNC			
particle(TEMPO)	—	145 ±31	—
film	5–10	—	0.04–0.07
BC			
particle	—	78 ±17	—
film	10–35	—	0.087–0.51

***E* = Young's modulus. E_A= elastic modulus in axial direction. σ_f = tensile strength (tensile testing).**

The properties of the processed microfibrils– the morphology, crystallinity, and aspect ratio – are governed by a variety of processing methods for pre-treatments and disintegration.[6]

There are several other disintegration methods besides the TEMPO reaction, such as mechanical, acid hydrolysis, and enzymatic hydrolysis treatment. For mechanical treatments, for example, high pressure homogenization, high intensity ultrasonication, or microfluidization is utilized to produce cellulose fibrils from wood fiber (WF), plant fiber (PF), microcrystalline cellulose (MCC), bacteria, algae, and tunicate.[6] These techniques generate intense shear, splitting

the fibers into long and flexible microfibrils along the longitudinal axis. The resultant fibrils are known as microfibrillated (MFC) or nanofibrillated cellulose (NFC).

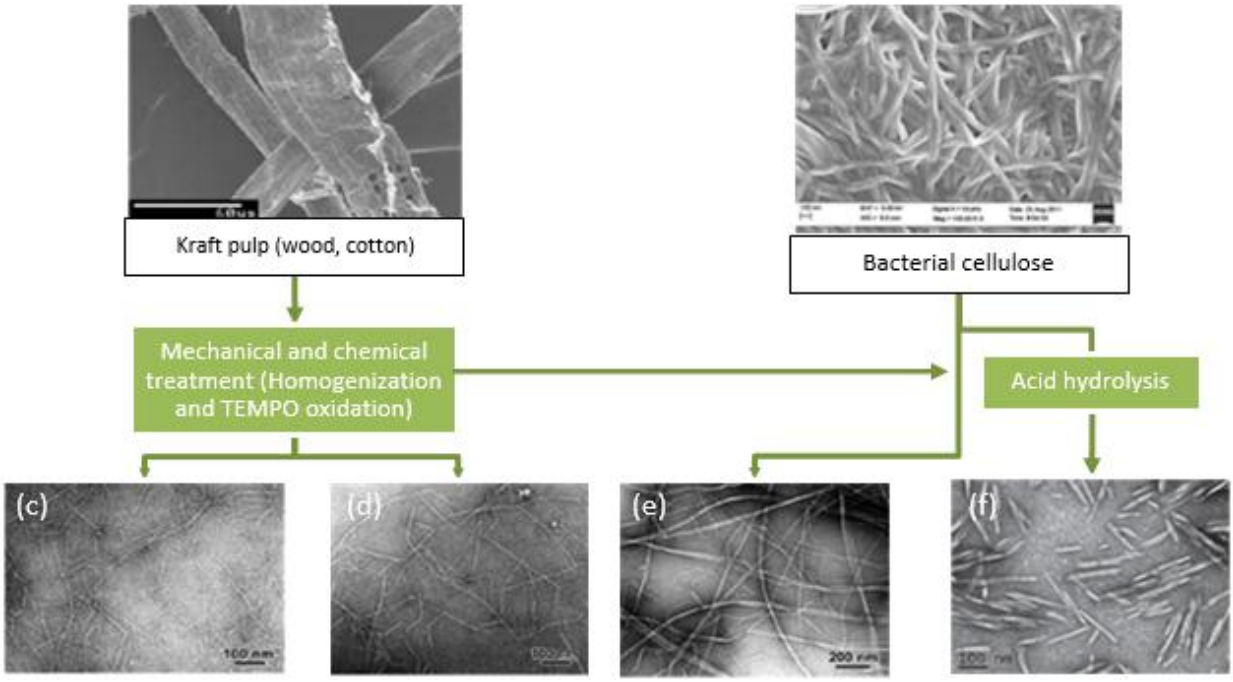

Figure 3. Scanning electron micrographs of (a) kraft pulp and (b) bacterial cellulose; transmission electron micrographs of nanofibrillated (c) wood, (d) cotton, (e) bacterial cellulose (NFC), and (f) bacterial cellulose nanocrystals (CNC)[1, 25]

Although the mechanical treatment helps to extract fibrils, having them long in length and uniform in diameter, the mechanical damage to crystalline structures should be carefully considered because it might lower the percent of crystallinity.[6]

Acid hydrolysis of natural fiber pulps allows for the formation of cellulose nanocrystals (CNC).[25]Zimmerman et al. adopted an acid hydrolysis process before homogenizing the sulfite pulps. Sulfuric acid was added to the oven dried pulps to hydrolyze, and 0.1M sodium hydroxide was subsequently used to neutralize the hydrolyzed pulps, followed by homogenization with a microfluidizer.[26] As a result, the treated pulps with the combination of acid hydrolysis and mechanical treatment had smaller widths than MFC with applied mechanical treatment only.

Additionally, the aspect ratios of CNC are not as high as that of MFC[25] since the fractional hydrolysis dissolves amorphous regions preferentially.[27]

Furthermore, Henriksson et al. applied enzymatic hydrolysis and employed pure C-type endoglucanase to disintegrate cellulosic wood fiber pulps.[28] The enzymatic treatment has been considered to be an environmentally-safe method since toxic solvents or chemical reactants were not used. The enzymatically treated MFC resulted in a higher aspect ratio than the one obtained from acid hydrolysis treatment.

3. TEMPO (2,2,6,6-tetramethylpiperidine-1-oxyl)

One of the objectives of this study is to disintegrate celluloses into more individualized nanofibrils with higher aspect ratios, reducing the energy input. TEMPO and its analogues are included in a group of compounds, also known as nitroxyl or nitroxide radicals as shown in Figure4.

Figure 4. Chemical structures of radical nitroxyl compounds: (A) 2,2,6,6-tetramethylpiperidine-N-oxyl, (B) 2,2,5,5-tetramethylpyrrolidine-N-oxyl, and (C) 4,4-dimethyloxazolidine-N-oxyl[29]

The outstanding characteristicsof the nitroxyl radicals are that they show high stability due to delocalization of the unpaired electron.[30] In addition, hydrogens next to the α-carbon give rise to instability,[29] but the absence of those hydrogens around N-O bond provides stability. Therefore, TEMPO and nitroxyl radicals are suitable for a variety of applications owing to its stability and selectivity.[29]

Figure 5. Mechanism of TEMPO regioselective oxidation of cellulose nanofibrils (adapted from Ref. 30; fair use; Isogai, A.; Saito, T.; Fukuzumi, H., TEMPO-oxidized cellulose nanofibers. Nanoscale 2011, 3 (1), 71-85.)

The TEMPO-mediated oxidation method selectively converts the C6 primary hydroxyl groups of cellulose to aldehyde or carboxylic acid with sodium hypochlorite (NaClO) as a primary oxidant. TEMPO and sodium bromide (NaBr) are used as catalysts. At pH 10, the optimal conditions are achieved for TEMPO-catalyzed oxidation.[7] The mechanism stated above is depicted in Figure 5. Consequently, polyuronic acids, having carboxyl groups, are generated.[6]During this oxidation reaction, 2 mol of NaClO are required to modify 1 mol of primary hydroxyl group to 1 mol of carboxylate group via the aldehyde. The amount of NaClO in the medium and the oxidation time are proportional to the final concentration of carboxylate groups.[31]The TEMPO-catalyzed oxidation is considerably beneficial to disintegrate cellulose fibrils by weakening the interfibril interactions among nanofibrils; it applies the negative electrostatic repulsion to the fibrils by the introduction of appreciable amounts of carboxylate moieties, keeping them apart from each other.[29] It is also used in combination with a routine

kitchen blender treatment for better dispersion.[2]As a result, TEMPO-oxidized cellulose consists of long and flexible nanofibrils, which have various functional groups on their surface, such as carboxyl, hydroxyl, and aldehyde.[27] Furthermore, TEMPO-mediated oxidation gives rise to nanofibrils with 3-4 nm width and several micrometers in length.[7] The homogenized fibrils present transparent suspensions because the fibrils are thinner than the wavelength of the light.[1,27] Thus, more transparent suspensions can be obtained as the degree of oxidation increases.

However, according to the result of ^{13}C NMR and other analyzing techniques, it has been reported that such modification is largely present on the surface of the cellulose fibrils. Since oxidation does not occur inside of the cellulose fiber, that is in crystalline regions, TEMPO-mediated oxidation does not have a significant effect on the fibrous morphology and crystallinity at the micron scale.[31] Even with an exceptionally high amount of primary oxidant (about 10 mmol NaOCl/g cellulose), no change in crystallinity was detected.[23]

2.4. Graphene Oxide (GO)

Graphene consists of carbon atoms in a 2-dimensional honey-comb structure as presented in Figure 6. The sp^2-hybridized carbon network exhibits excellent mechanical, thermal, and electrical properties. In addition, graphene is known as the thinnest nanofiller, having only 0.34 nm of the theoretical thickness in a singular flat sheet based on the atomic layer spacing of graphite, which is 0.68 nm.[32] Graphene oxide – one of the derivatives of graphene – has been widely used for nanocomposite fabrication. Graphene oxide has high polarity due toitsoxygen-containing functionalities, such as hydroxyl, carboxyl, epoxide, and carbonyl groups. A high density of hydroxyl and epoxide groups is attached to the basal plane of graphene; carboxyl groups are observed at the edges of the plane. Carbon and oxygen atoms exist approximately in

the ratio of 2 to 1, and the oxidized components cover 60-70% of the surface of the carbon plane.[32] The thickness of graphene oxide is theoretically about 0.7-0.8 nm, which is two times thicker than that of the normal graphene owing to the high amount of functional groups generated by the oxidation treatment. Graphene oxide also shows slightly negative charges by the addition of anionic carboxylate groups.[32]

Figure 6. Schematic representation of (A) graphene and (B) graphene oxide

Due to its high potential for formation of strong intermolecular interactions with the polymer matrix, graphene oxide is a good candidate as a nanofiller in nanocomposite fabrication. The Young's modulus of an individual graphene oxide sheet is about 250 GPa.[33]The interaction of graphene is solely constrained to weak van der Waals forces, π-π stacking, and hydrophobic-hydrophobic interactions, whereas graphene oxide is additionally capable of forming hydrogen bonds due to the abundant polar functionalities. In this regard, the graphene oxide sheet and polymer matrix nanocomposites coupled with hydrogen bonds form interactions as strong as the covalently crosslinked ones.[32] Another significant feature of graphene oxide is its amphiphilicity. Graphene oxide is composed of a heterogeneous surface containing hydrophobic graphitic and hydrophilic oxidized regions.[34]

The favorable characteristic of graphene oxide as a nanofiller is that it can be combined with either hydrophilic or hydrophobic polymers. In order to reach the desired properties,

graphene oxide should be incorporated in the polymer matrices homogeneously, forming strong intermolecular interactions between nanofillers and matrices. In other words, the ultimate mechanical properties, such as stiffness, toughness, and elongation of the fabricated nanocomposite are governed by dispersionon a molecular scale and affinity of the nanofillersfor the polymer matrix.[32]Ultimately, the incorporation of graphene oxide is expected to improve the thermal, mechanical, and barrier properties for industrial applications.

2.5. NFC/GO nanocomposites

The fibrillated nanocelluloses obtained by different mechanical or chemical treatments were mixed with graphene oxide nanosheets, constructing a hydrogen bonding network as shown in Figure 7. The prevalent ways to prepare nanocellulose film are a simple solvent casting of nanocellulose suspension on a proper surface, and extrusion of freeze-dried cellulose.[25] In this study, a solution casting method was adopted to prepare a graphene oxide/TEMPO-mediated cellulose nanocomposite film since it is efficient to impart the change in formation of hydrogen bonds between the incorporated nanofillers and polymer matrices. Accordingly, designing and developing such novel nanocomposites has great potential since they can be used for myriad industrial applications, such as papers, aerogels, hydrogels, and transparent films.[25]

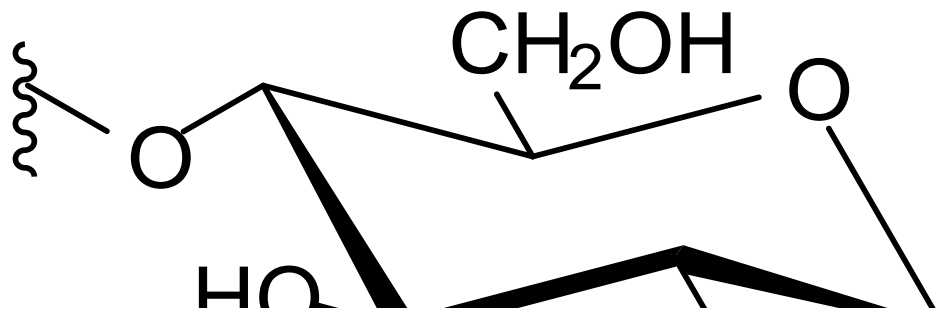

Figure 7. General representation of fabrication of TEMPO-mediated cellulose/GO nanocomposites. NFC prepared via TEMPO-mediated oxidation mixed with the GO solution, followed by homogenization

2.6. Characterization of Cellulose Nanocomposites

Understanding the characteristics of the fabricated nanocomposites is as crucial as designing the composites. Characteristics, such as chemical structures, crystalline, thermal, tensile, barrier properties have a significant impact on the final products. Therefore, analyzing the properties of the reinforced nanofibrillated film in this study plays a decisive role for industrial applications.

Several complementary techniques have been utilized – Fourier transform infrared spectroscopy (FTIR), differential scanning calorimetry (DSC), thermogravimetric analysis(TGA), scanning electron microscopy (SEM), X-ray powder diffraction (XRD), dynamic mechanical analysis (DMA), water vapor transmission rate (WVTR), oxygen transmission rate (OTR). FTIR is used to see the hydrogen bonds between graphene oxide and cellulosic polymer matrix; DSC is employed to observe the glass transition temperature (Tg), crystallization temperature (Tc), and melting temperature (Tm); TGA measures the onset of weight loss and thermal stability; SEM and XRD investigate the morphology and crystallinity of

nanocomposites, respectively; DMA measures mechanical properties, in particular, Young's modulus, storage modulus, loss modulus, and tensile strength. OTR and WVTR are used to observe a capability to resist the influx of gases and liquids.

REFERENCES

1. Saito, T.; Nishiyama, Y.; Putaux, J.-L.; Vignon, M.; Isogai, A., Homogeneous suspensions of individualized microfibrils from TEMPO-catalyzed oxidation of native cellulose. *Biomacromolecules* **2006,***7* (6), 1687-1691.
2. Berglund, L. A.; Peijs, T., Cellulose biocomposites—from bulk moldings to nanostructured systems. *MRS bulletin* **2010,***35* (03), 201-207.
3. Satyanarayana, K.; Sukumaran, K.; Mukherjee, P.; Pavithran, C.; Pillai, S., Natural fibre-polymer composites. *Cement and Concrete composites* **1990,***12* (2), 117-136.
4. Rong, M. Z.; Zhang, M. Q.; Liu, Y.; Yang, G. C.; Zeng, H. M., The effect of fiber treatment on the mechanical properties of unidirectional sisal-reinforced epoxy composites. *Composites Science and technology* **2001,***61* (10), 1437-1447.
5. Dufresne, A., Cellulose-based composites and nanocomposites. *Monomers, polymers and composites from renewable resources* **2008**, 401-418.
6. Moon, R. J.; Martini, A.; Nairn, J.; Simonsen, J.; Youngblood, J., Cellulose nanomaterials review: structure, properties and nanocomposites. *Chemical Society Reviews* **2011,***40* (7), 3941-3994.
7. Siqueira, G.; Bras, J.; Dufresne, A., Cellulosic bionanocomposites: a review of preparation, properties and applications. *Polymers* **2010,***2* (4), 728-765.
8. Babu, V.; Thapliyal, A.; Patel, G. K., *Biofuels production*. John Wiley & Sons: 2013.
9. Azizi Samir, M. A. S.; Alloin, F.; Dufresne, A., Review of recent research into cellulosic whiskers, their properties and their application in nanocomposite field. *Biomacromolecules* **2005,***6* (2), 612-626.
10. Brännvall, E., Aspects on strength delivery and higher utilisation of the strength potential of softwood kraft pulp fibres. *Royal Institute of Technology: Stockholm, Sweden* **2007**.
11. Kar, K. K.; Rana, S.; Pandey, J., *Handbook of polymer nanocomposites. Processing, performance and application*. Springer: 2015.
12. John, M. J.; Thomas, S., Biofibres and biocomposites. *Carbohydrate polymers* **2008,***71* (3), 343-364.
13. Andresen, M.; Johansson, L.-S.; Tanem, B. S.; Stenius, P., Properties and characterization of hydrophobized microfibrillated cellulose. *Cellulose* **2006,***13* (6), 665-677.
14. Dufresne, A.; Cavaille, J.-Y.; Vignon, M. R., Mechanical behavior of sheets prepared from sugar beet cellulose microfibrils. *Journal of applied polymer science* **1997,***64* (6), 1185-1194.
15. Stenstad, P.; Andresen, M.; Tanem, B. S.; Stenius, P., Chemical surface modifications of microfibrillated cellulose. *Cellulose* **2008,***15* (1), 35-45.
16. Bouvier, E. S.; Koza, S. M., Advances in size-exclusion separations of proteins and polymers by UHPLC. *TrAC Trends in Analytical Chemistry* **2014,***63*, 85-94.
17. Habibi, Y.; Lucia, L. A.; Rojas, O. J., Cellulose nanocrystals: chemistry, self-assembly, and applications. *Chemical reviews* **2010,***110* (6), 3479-3500.
18. Festucci-Buselli, R. A.; Otoni, W. C.; Joshi, C. P., Structure, organization, and functions of cellulose synthase complexes in higher plants. *Brazilian Journal of Plant Physiology* **2007,***19* (1), 1-13.
19. Lu, J.; Askeland, P.; Drzal, L. T., Surface modification of microfibrillated cellulose for epoxy composite applications. *Polymer* **2008,***49* (5), 1285-1296.

20. Lepoutre, P.; Hui, S.; Robertson, A., Some Properties of Polyelectrolyte-G rafted Cellulose. *Journal of Macromolecular Science—Chemistry* **1976,***10* (4), 681-693.
21. Herrick, F. W.; Casebier, R. L.; Hamilton, J. K.; Sandberg, K. R. In *Microfibrillated cellulose: morphology and accessibility*, J. Appl. Polym. Sci.: Appl. Polym. Symp.;(United States), ITT Rayonier Inc., Shelton, WA: 1983.
22. Turbak, A. F.; Snyder, F. W.; Sandberg, K. R. In *Microfibrillated cellulose, a new cellulose product: properties, uses, and commercial potential*, J. Appl. Polym. Sci.: Appl. Polym. Symp.;(United States), ITT Rayonier Inc., Shelton, WA: 1983.
23. Saito, T.; Isogai, A., TEMPO-mediated oxidation of native cellulose. The effect of oxidation conditions on chemical and crystal structures of the water-insoluble fractions. *Biomacromolecules* **2004,***5* (5), 1983-1989.
24. Zimmermann, T.; Bordeanu, N.; Strub, E., Properties of nanofibrillated cellulose from different raw materials and its reinforcement potential. *Carbohydrate Polymers* **2010,***79* (4), 1086-1093.
25. Wei, H.; Rodriguez, K.; Renneckar, S.; Vikesland, P. J., Environmental science and engineering applications of nanocellulose-based nanocomposites. *Environmental Science: Nano* **2014,***1* (4), 302-316.
26. Zimmermann, T.; Pöhler, E.; Geiger, T., Cellulose fibrils for polymer reinforcement. *Advanced engineering materials* **2004,***6* (9), 754-761.
27. Johnson, R. K.; Zink-Sharp, A.; Renneckar, S. H.; Glasser, W. G., A new bio-based nanocomposite: fibrillated TEMPO-oxidized celluloses in hydroxypropylcellulose matrix. *Cellulose* **2009,***16* (2), 227-238.
28. Henriksson, M.; Henriksson, G.; Berglund, L.; Lindström, T., An environmentally friendly method for enzyme-assisted preparation of microfibrillated cellulose (MFC) nanofibers. *European Polymer Journal* **2007,***43* (8), 3434-3441.
29. Bragd, P.; Van Bekkum, H.; Besemer, A., TEMPO-mediated oxidation of polysaccharides: survey of methods and applications. *Topics in Catalysis* **2004,***27* (1-4), 49-66.
30. Hicks, R. G., What's new in stable radical chemistry? *Organic & biomolecular chemistry* **2007,***5* (9), 1321-1338.
31. Saito, T.; Kimura, S.; Nishiyama, Y.; Isogai, A., Cellulose nanofibers prepared by TEMPO-mediated oxidation of native cellulose. *Biomacromolecules* **2007,***8* (8), 2485-2491.
32. Hu, K.; Kulkarni, D. D.; Choi, I.; Tsukruk, V. V., Graphene-polymer nanocomposites for structural and functional applications. *Progress in Polymer Science* **2014,***39* (11), 1934-1972.
33. Gómez-Navarro, C.; Burghard, M.; Kern, K., Elastic properties of chemically derived single graphene sheets. *Nano letters* **2008,***8* (7), 2045-2049.
34. Kim, J.; Cote, L. J.; Kim, F.; Yuan, W.; Shull, K. R.; Huang, J., Graphene oxide sheets at interfaces. *Journal of the American Chemical Society* **2010,***132* (23), 8180-8186.

CHAPTER 3. TEMPO-oxidized Nanofibrillated Cellulose Film (NFC) incorporating Graphene Oxide (GO) Nanofillers

3.1. Abstract

To design a new system of TEMPO-oxidized cellulose nanofibrils (TOCNs)/graphene oxide (GO) composite, the 2,2,6,6-tetramethylpiperidine-1-oxyl radical (TEMPO)-mediated oxidation was utilized to disintegrate never-dried wood nanofibrillated cellulose (NFC). GO was incorporated through high intensity homogenization and ultrasonication with varying degree of oxidation (0.5X, 1X, and 2X) and GO percent loadings: 0.4, 1.2, and 2.0wt %. As a result, despite the presence of carboxylate groups and graphene oxide (GO), X-ray diffraction (XRD) test showed the crystallinity of the bio-nanocomposite was not altered. Scanning electron microscopy (SEM) was used to characterize morphology. In addition, the thermal stability of TOCN/GO composite decreased with increasing oxidation level, and dynamic mechanical analysis (DMA) showed strong intermolecular interactions with improvement in Young's storage modulus, and tensile strength, compared to neat NFC. Fourier transform infrared spectroscopy (FTIR)was employed to see the hydrogen bonds between GO and cellulosic polymer matrix. The oxygen transmission rate (OTR) of TOCN/GO composite decreased after the treatment. The water vapor permeability (WVP) was not significantly affected by the reinforcement with GO, but the moderate oxidation enhanced the barrier properties. Ultimately, the newly fabricated TOCN/GO composite can be utilized in a wide range of life science applications, such as food and medical industries.

3.2. Introduction

Industries and manufacturers recently have sought to substitute petroleum-based plastics with eco-friendly biocomposites for sustainable applications. Nanocomposites fully derived from biomaterials have received attention due to their biodegradability, biocompatibility, and renewability, combined with commercial viability. For example, the potential biopolymers, such as cellulosic plastics, starch plastics, soy-based plastics, and poly(lactic acid) (PLA), were used to fulfill those desired benefits.[1] In terms of the environmental and ecological aspects, the abundant biopolymer, cellulose, has been considered a promising material substituting traditional plastics. In this study, nanofibrillated cellulose (NFC) was used to fabricate nanocomposites as a good polymer matrix candidate. The stiffness of nanocellulose is smaller by only one order of magnitude than that of carbon nanotubes, and it shows high elastic modulus at 138 GPa.[2]

Cellulose fibrils, ranging from 10 to 100 nm in width, are generally produced via two main processes: mechanical refining and high pressure homogenization of natural pulps.[3] In spite of the high energy input by intense mechanical treatment, the complete isolation of cellulose fibril bundles is not attainable owing to abundant hydrogen bonds tightly linking the fibrils.[4-5] To achieve further individualization of nanofibrils, a promising chemical disintegration method is commonly used via 2,2,6,6-tetramethylpiperidine-1-oxyl (TEMPO) regioselective oxidation by converting primary alcohols to aldehydes and carboxylate groups. Sodium bromide (NaBr) is commonly used as a catalyst and sodium hypochlorite (NaClO) as a primary oxidant for *in-situ* reaction of the TEMPO radicals under mild conditions.[6] The surface modified cellulose becomes disintegrated by applying negative electrostatic repulsions and loosening the cohesiveness between microfibrils and ends up with transparent nanofibrils. These ranges from 3 to 5 nm in width and several microns in length.[6] TEMPO-mediated oxidation of cellulose introduces the

carboxylate groups at their surfaces only. This phenomenon is attributed to the large crystalline regions and poor accessibilities to the fibrils inside. Nevertheless, TEMPO-mediated oxidation yields a dense network of nanofibrils, providing a good distribution in water due to abundant functional groups at certain hydrophilic portions.

In the present study, the excellent polymer matrix is fabricated with nanofillers to construct nanocomposites. In recent years, the incorporation of nanofillers, such as organoclay, cellulose nanocrystals, carbon nanotubes (CNT), graphene oxide, and polysilsesquioxane, has been widely used to attain the desired properties - mechanical and barrier properties.[7] Of the many nanoparticles, herein, graphene oxide-reinforced composites were developed. Graphene is composed of the sp^2-hybridized carbon network and exists in a 2-dimensional honeycomb structure. However, graphene oxide (GO) layers have abundant oxygen-containing functional groups – hydroxyl, epoxy, carbonyl, and carboxyl, so that it is prone to be dispersed homogeneously in an aqueous medium and form intermolecular interactions between nanofillers and polymer matrices at a molecular level.[8]GO is one of the extensively used nanofillers into a polymer matrix because it shows excellent thermal, mechanical, and electrical properties. Due to the significant property enhancement even with the low GO content, the fabrication of microcrystalline cellulose (MCC)/GO nanocomposites has also been reported in another study.[8] In order to satisfy the targeted properties, a uniform dispersion of nanofillers in the polymer matrix is considered as a major factor; however, the strong intra- and inter-molecular interactions of cellulose fibrils and van der Waals forces of GO itself might hinder the efficient intermolecular cohesiveness of two phases. Therefore, optimized and proper mechanical and chemical treatment should be applied for the sufficient load transfer from the polymer matrices to graphene oxide.[8]

The hypothesis of this study is that the well-dispersed graphene oxide (GO) nanofillers and TEMPO-oxidized cellulose matrix, composed of disintegrated fibrils, form TOCN/GO nanocomposites, which would have a significant effect on barrier, mechanical, and viscoelastic properties. Therefore, the objective of this research is to obtain homogeneous dispersion, preventing the aggregation of graphene oxide (GO) in the TEMPO-oxidized cellulose by disintegrating fibrils to the greatest extent and to investigate the effect of the GO content and degree of oxidation (TEMPO) in the TOCN/GO nanocomposites. They were then analyzed by X-ray diffraction (XRD), Fourier transform infrared spectroscopy (FTIR), water vapor (WVTR) and oxygen transmission rate (OTR), dynamic mechanical analysis (DMA), field emission scanning electron microscopy (FESEM), thermogravimetric analysis (TGA), and tensile testing to understand various properties. The resulting nanomaterial can be applied in the field requiring high barrier and mechanical performance, such as coating, composites reinforcement, packaging, and drug delivery; furthermore, it could be a potential nanomaterial as absorbents to remove organic pollutants and oils dispersed in water.[9,10]

3.3. Materials and Methods

3.3.1. Materials

Never-dried nanofibrillated cellulose, made from northern bleached softwood kraft pulp, with ~ 3% consistency (dry pulp/slurry) and 28.4 μm in width were purchased from University of Maine and used for further treatment. 2,2,6,6-Tetramethylpiperidine-1-oxyl (TEMPO, 98%, Sigma-Aldrich), sodium hypochlorite (NaClO,13%, Fisher Scientific), sodium bromide (NaBr, 99+%, reagent grade, Sigma-Aldrich), hydrochloric acid (HCl, 0.1 N, Certified, Fisher Scientific), sodium hydroxide (NaOH, 0.1N,Certified, Fisher Scientific), and ethanol (C_2H_6O,

95%, Decon Labs) were used as received. Graphite (particle size of < 20 μm) was obtained from Sigma Aldrich, USA.

3.3.2. Preparation of exfoliated graphene oxide

A modified Hummers method was used to prepare exfoliated graphene oxide from graphite.[11] 10 g of graphite powder was added to 250 mL of sulfuric acid (H_2SO_4)in a flask at room temperature. The mixture was placed in an ice bath and followed by the addition of 35 g of potassium permanganate ($KMnO_4$), which was then allowed to react at 35 °C for 12 h. The solution was cooled to < 5 °C in an ice bath again. Excess hydrogen peroxide (H_2O_2) was gradually added to the flask with stirring to reduce unreacted $KMnO_4$. Once the mixture turned bright yellow and bubbles were observed, it was washed repeatedly with distilled water until a pH of 7 was achieved. The resulting mixture was transferred to a conical centrifuge tube and centrifuged until no more supernatant was observed. Lastly, liquid nitrogen was utilized to freeze the neutralized graphene oxide, which was subsequently obtained in powder form via freeze drying. The exfoliated graphene oxide was characterized by XRD and stored in a vacuum desiccator.

3.3.3. TEMPO-Mediated Oxidation of Cellulose

Cellulose (20g) was suspended in distilled water (2 L) using a domestic blender. 0.25 g of TEMPO and 2.5 g of sodium bromide (1X TEMPO) were added to a 3000 mL three-neck round bottom flask, and the mixture was agitated with an overhead stirrer at 300 rpm. For 0.5X TEMPO and 2X TEMPO, the amount of TEMPO and NaBr were reduced in half (0.125 g, TEMPO and 1.125 g NaBr) and doubled (0.5 g, TEMPO and 5 g, NaBr), respectively. Then, 46

mL of 13% sodium hypochlorite (NaClO, 4.459 mmol/g cellulose) was gradually added to the cellulose slurry with a syringe pump at a rate of 1500 μL/min at room temperature. The pH of the solution was maintained to be 10±2 by the drop-wise addition of 0.5 N NaOH. Once no further change in pH was detected, 150 mL of ethanol was added to completely quench the oxidation reaction. The oxidized cellulose was washed thoroughly with distilled water by centrifugation at 5000 rpm for 30 minutes at 0-5 °C. This process was repeated several times until the pH of the cellulose sediment after the washes was adjusted to 7. The TEMPO-oxidized cellulose was stored at 4 °C for further treatment. The TEMPO- oxidized cellulose nanocomposites prepared at different oxidation levels (0.5X, 1X, and 2X TEMPO) without GO were denoted as 0.5X, 1X, and 2X TOCN, respectively.

3.3.4. Preparation of TOCN/GO nanocomposites

TEMPO-oxidized cellulose was mixed with graphene oxide (GO) with a high-pressure laboratory homogenizer (MINI DeBEE). The TOCN/GO solutions of the different concentrations were continuously agitated and homogenized five times using a 200-μm nozzle. The TEMPO- oxidized cellulose nanocomposites were prepared with the addition of various graphene oxide percent loadings: 0.4, 1.2, and 2.0 wt % with respect to dried cellulose, which are denoted as TOCN/GO-0.4, TOCN/GO-1.2, and TOCN/GO-2.0, respectively. The water content of the TEMPO-GO dispersions was evaluated in a moisture analyzer (OHAUS model MB45) in triplicate. Nanocomposite films were then cast from the cellulose/GO suspensions on a petri dish at 50% RH and room temperature.

3.4. Characterization

3.4.1. Determination of Carboxylate and Aldehyde Contents

Conductometric titration

The electric conductivity titration method verified carboxylate content of the TEMPO-oxidized cellulose. A dried cellulose sample (0.4 g) was mixed with 0.1N hydrochloric acid (100 mL) for an hour to protonate all the carboxyl groups. 0.1 N NaOH (95 mL) was added, and the solution was adjusted to 300 mL with deionized water. The mixture was then titrated with 0.1 N NaOH solution. Carboxylate contents were determined on a Metrohm 905 Titrandoand calculated from the equation,

$$\text{carboxylate groups (mmol/g)} = \frac{c\ x\ v}{m} = \frac{c(v_2 - v_1)}{m}$$

where c is the molar concentration of NaOH (in M), m is the mass of the solid cellulose sample (in g), and v is the difference between the volume of NaOH (in mL) consumed to neutralize the excess hydrochloric acid and carboxylic acid.[12] The measurements were repeated in triplicate.

3.4.2. Fourier transform infrared spectrometry (FT-IR)

FTIR spectra of TOCN-GO composite films were recorded on a Nicolet 8700 FT-IR Spectrometer using the attenuated total reflection (ATR) method. The data was collected from 4000 to 500 cm^{-1} with 64 scans at a resolution of 4 cm^{-1}. A background spectrum was also collected before each sample.

3.4.3.X-ray diffraction analysis (XRD)

The crystalline morphology of TOCN/GO nanocomposite was analyzed on a Bruker D8 XRD at room temperature using Cu-Ka (wavelength, 0.15406 nm) radiation conducting at 40 kV and 40 mA. The diffraction data was collected from the 2Θ range of 5 to 60° with a scanning rate of 4°/min. The baseline correction was automatically applied for a better comparison, and percent crystallinity ($\%\chi_c$) of each sample was calculated by the following equation.

$$\chi_c(\%) = \frac{Total\ area\ of\ crystlline\ \ peaks}{Total\ area\ of\ all\ peaks} \text{ x } 100\%$$

3.4.4. Dynamic mechanical analysis (DMA)

Dynamic mechanical analysis was carried out on a Q800 DMA in the tension mode. Specimens with 20 ± 0.5 mm length and 5.0 ± 0.1 mm width were used. The storage modulus (G′) and the loss modulus (G″) were investigated as a function of increasing temperature, ranging from 0 to 150 °C at a heating rate of 5 °C/min. Preload force and amplitude of 0.01 N and 20 μm, respectively, were used during the test.

3.4.5 Mechanical testing

The mechanical properties, such as tensile strength and Young's modulus were determined on the TA-XT 32 texture analyzer from Texture Technologies. Specimens with at least 50 mm length and 15 mm width were measured at 6 mm min^{-1} and a 10 mm gauge length under ambient temperature conditions. Five replicates for each specimen were measured and normalized by thickness, and its average value was calculated. All of the films were stored in a humidity control chamber at RH 50% for 48 hours before each use.

3.4.6 Morphological analysis

The field emission scanning electron microscopy (FESEM) was carried out on a LEO (Zeiss) 1550 operated with an acceleration voltage of 2 kV. The cross-section of the sample was obtained by fracturing it in liquid nitrogen to assess the cross-sectional morphology. The TOCN/GO nanocomposite films were coated by sputtering with a thin layer of iridium.

3.4.7. Water permeation analysis

Water vapor transmission rate (WVTR) was determined to measure the volume of water vapor diffusing through a film per unit area and time using i-Hydro 7500 water vapor transmission rate testing system (Labthink International, Inc., U.S.A.). All the specimens were conditioned at 50% relative humidity before each test. The edges of the specimens were masked using aluminum foil tape (average thickness of 30 ± 3 μm and test dimension of 2.5 X 2.5 cm). The WVTR of TOCN/GO nanocomposite films were measured in triplicate and a standard mode (4 cycles) at 50% RH and 23.5 °C. The flow rate of the N2 purge and humidified gas for each cell were adjusted to 100±2 ml/min. The WVTR was normalized by the partial pressure difference and thickness to obtain the water permeation coefficient.

3.4.8 Gas permeation analysis

The oxygen transmission rate (OTR) of TOCN and GO composite were determined using an oxygen analyzer (OxySense 5250i) under ambient temperature conditions with 0% relative humidity. The gas permeation chamber was divided into two wells by the sample film. Pure nitrogen (a carrier gas) and oxygen (a test gas) were purged into the sensing well and the driving

well with a flow rate of 1 mL/min. At least three replicates for each specimen were masked using aluminum foil tapes (average thickness of 30 ± 3 μm and test dimension of 1.5 X 1.5 in.) were measured. The OTR was collected every five minutes and stopped once the oxygen concentration reached the steady state, a regression coefficient of 0.99 or higher. Each sample was preconditioned in a vacuum oven at the desired 50% RH for 48 hours.

3.4.9 Thermal gravimetric analysis (TGA)

TGA was conducted on a TA Q500 TGA to observe the thermal degradation behavior of the TOCN-GO nanocomposites as the effect of the oxidation state and GO content. Approximately 10 mg of samples were heated from the room temperature to 700 °C at a rate of 10 °C/min under nitrogen.

3.5. Results and Discussion

3.5.1 Surface charge of neat NFC and TOCN/GO nanocomposites

The C6 primary hydroxyl groups were converted to carboxylate groups via NaClO/NaBr/TEMPO oxidation at three different TEMPO and NaBr catalyst levels. It was measured by conductometric titration based on the consumed amounts of NaOH. As shown in Table 1, the charge densities of neat NFC, 0.5X, 1X, 2X TOCN, related to carboxyls, were 0.183, 0.280, 0.370, and 0.425 mmol per g of cellulose, respectively.

Table 1. Carboxylate content with different concentration of catalysts

Sample	NaClO (mmol/g)	NaBr (g)	TEMPO (g)	Carboxylate (mmol/g)
neat NFC	-	-	-	0.183
0.5X TOCN	4.46	1.25	0.125	0.280
1X TOCN	4.46	2.5	0.25	0.370
2X TOCN	4.46	5	0.5	0.425

In the presence of an excess of NaClO, the amounts of TEMPO/NaBr catalysts are quite proportional to that of the converted C6 carboxyls of cellulose, providing a correlation coefficient R^2=0.91. The linear relationship between TEMPO/NaBr quantities and surface charge densities is also confirmed by Marjasvaara et al., and they found that a doubled amount of TEMPO generates the corresponding carboxyls.

3.5.2. Dispersion of GO fillers in a TOCN matrix

Intermolecular Interaction in FTIR spectra of TOCN/GO composites

In the present study, FTIR was used to investigate the presence of graphene oxide and to determine the degree of oxidation by comparing the peak intensities. The FTIR spectra of neat NFC, neat GO, and TOCN-GO composites with various GO contents are displayed in Figure 1(a).

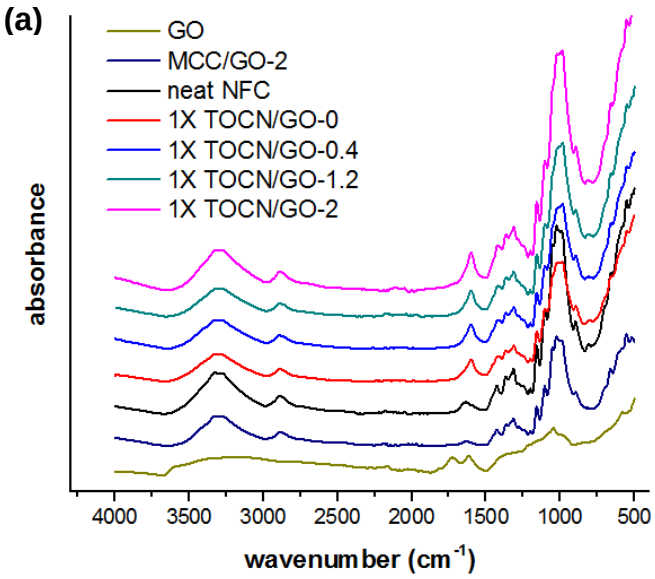

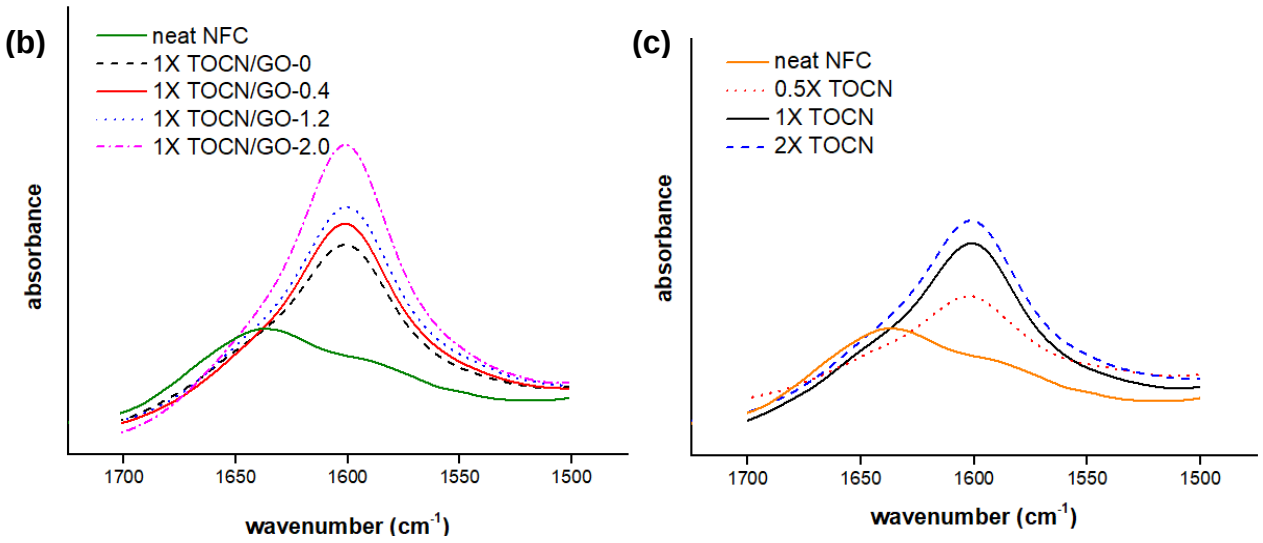

Figure 1. Stacked FTIR spectra of neat NFC and TOCN/GO composites (a) and FTIR absorption spectra of 1X TOCN/GO with various GO loadings (b) and TOCN films with different degree of oxidation (c) at 1600 cm^{-1}

It is evident that the broad and strong peaks centered at 3330 and 2890 cm^{-1} are relevant to the stretching of the hydroxyl groups and carboxylate groups, respectively. The broad region corresponding to carboxylate groups also overlap with the absorption of C-H stretching.[13] In addition, the characteristic absorption at 1630 cm^{-1} is indicative of stretching vibrations of carboxylate groups. This result is quite in accordance with that reported by Mandal et al. The spectrum of CMC (carboxymethyl cellulose) shows intense peaks at 2917 and 1631 cm^{-1}, corresponding to stretching vibration of C-H and carboxylate groups.[14] Other finger print absorptions of $-CH_2$ scissoring, -OH bending, and C-O-C pyranose ring vibration are detected at 1430, 1373, and 1030 m^{-1}, respectively.[15]As presented in Figure 1(a), the FTIR spectrum of GO represents a broad peak at 3183 cm^{-1}, which corresponds to the hydroxyl groups, and the peaks at 1729 and 1616 are associated with C=O and C=C stretching vibrations, respectively.[16]The peak assigned for C=O stretching vibration of GO, in general, should be detected around 1730 cm^{-1}, but it was overlapped with the carboxylate moieties region. Additionally, most of the spectral features of TOCN/GO composites are analogous except for the intensity of the peaks as shown in

Figure 1(b). For example, the higher absorbance at 1630 cm^{-1} in the spectra confirms the increased GO loadings in TOCN/GO nanocomposites due to the introduction of more oxygen-containing groups introduced. This observation is in compliance with the characteristic absorption spectra obtained by Shao et al.[17] In addition to the findings from Shao et al, this study found that the peak at 1630 cm^{-1}, which is associated with the stretching vibration of carboxylate groups, showed higher intensities as the degree of oxidation became more apparent for 2X TOCN.[17] It is because the amount of carboxylate moieties converted from the C6 primary hydroxyls of cellulose increases as to the amount of TEMPO involved in the reaction.

3.5.3. Crystallinity of the TOCN/GO Nanocomposites

X-ray diffraction analysis was utilized to investigate the change of the degree of crystallinity upon the TEMPO oxidation and the inclusion of graphene oxide.

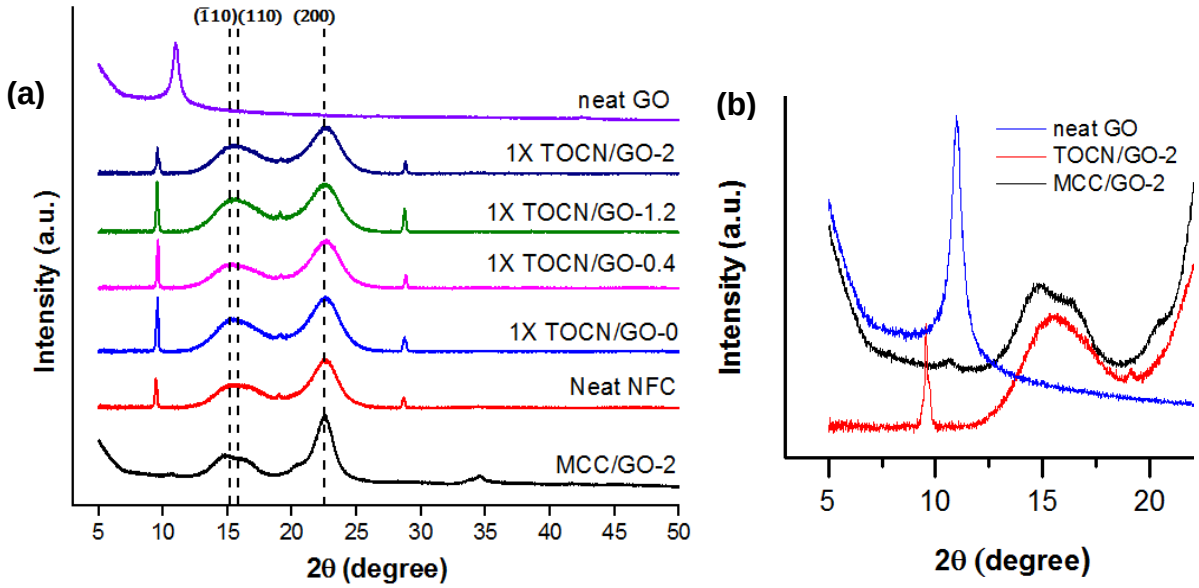

Figure 2. XRD patterns of neat NFC, GO, and TOCN/GO composites (a) and enlarged view of the XRD peak region of GO

As shown in Figure 2, the X-ray diffraction patterns of pristine NFC represent three characteristic peaks at 2Θ=15.4°, 16.6°, and 22.7°, assigned to the $(\bar{1}10)$, (110), and (200) planes

of the crystalline form of cellulose I, respectively.[9]The sharp intense peaks around 9.5°, 19.1°, and 28.7°, were also observed from the XRD spectra of pristine NFC films, which were assumed to be impurities of the as-received untreated nanocellulose. According to ^{13}C NMR and XRD spectra of the TEMPO-oxidized cotton linters, the carboxylate and aldehyde groups are largely presented at the C6 position of the cellulose surface and in non-crystalline regions of microfibrillated cellulose.[4] Correspondingly, Figure 2(a) illustrates that the characteristic intense peaks of all XRD profiles are very similar to each other although the width of each peak is slightly widened compared to the control. It indicates that neither TEMPO-mediated oxidation nor incorporation of GO highly affect the crystalline form. With respect to the crystallinity, the crystallinities of the native celluloses range from 59 to 92% depending on cellulose source materials.[18]

Table 2. Percent crystallinity (% *X*c) of the pristine NFC and TOCN/GO nanocomposites obtained by XRD

Sample	% X_c
neat NFC	60 (±1.0)
0.5X TOCN	62.3 (±3.5)
1X TOCN/GO-0	62.8 (±2.6)
1X TOCN/GO-0.4	61.7 (±3.4)
1X TOCN/GO-1.2	61.6 (±0.9)
1X TOCN/GO-2.0	62.3 (±5.9)
2X TOCN	61.8 (±2.4)

Table 2 displays that the percent of crystallinity derived from the ratio of the area of all crystalline peaks to the total area, was not significantly changed even with various amounts of TEMPO and the addition of GO as expected. For example, in the study from Saito et al., the percent crystallinity of neat spruce holocellulose was 59%, which was analogous to that of TEMPO-oxidized spruce holocellulose (60%).[18]Our result agrees with those of Saito et al. Despite the oxidation with 10 mmol/g cellulose of NaClO, a relatively high amount, the

crystallinity of cellulose and crystal size of cellulose I were almost identical.[4] Although it is conjectured that the increased amounts of carboxylate and aldehyde on the surface of cellulose I crystallites might attribute to this slight increase, this result substantiates that the TEMPO-mediated oxidation only occurs either on cellulose crystal surfaces or in the amorphous regions without any chemical modification inside of cellulose I crystallites.

In general, the exfoliation of graphene oxide is more facilitated compared to graphene and graphite in the polymer matrix,[2] but the strong van der Waals interactions might still cause the restacking, agglomeration, and heterogeneous dispersion even with the advanced mixing, especially, when the amount of nanoparticles reaches the critical loading.[19] Nevertheless, the well-distributed GO nanofillers were confirmed by XRD analysis. The homogeneous dispersion state can be proven by the absence of the (001) plane of graphene oxide, corresponding to the sharp peak observed at approximately 10.9°.[20]As shown in Figure 2(b), the XRD patterns of MCC (microcrystalline cellulose), which is physically mixed with 2% GO without further treatment,showed a small GO peak. It indicates that the GO nanoparticles were not successfully intercalated into the MCC matrix with physical mixing itself. Meanwhile, the peak around 10.9°was not observed in the XRD patterns of TOCN/GO-2. This phenomenon signifies that the mechanical and chemical TEMPO treatments applied here in the study played a significant role in exfoliation or complete separation of the graphene oxide sheets in the polymer matrix, not yielding the diffraction peak at 10.9°.

3.5.4. Viscoelastic properties ofthe TOCN/GO Nanocomposites

Figure 3(a) displays the logarithm of the storage modulus values as a function of temperature ranging from 0 to 150 °C. The storage modulus increased with increasing GO

loadings; however, it remained comparatively independent of temperature, ascribed to the high degree of crystallinity and hydrogen bonds.[21]Bulota et al. also addressed that the storage modulus of neat cellulose was not strongly affected by a temperature increase, resulting in a slight decrease in storage modulus only.[21]

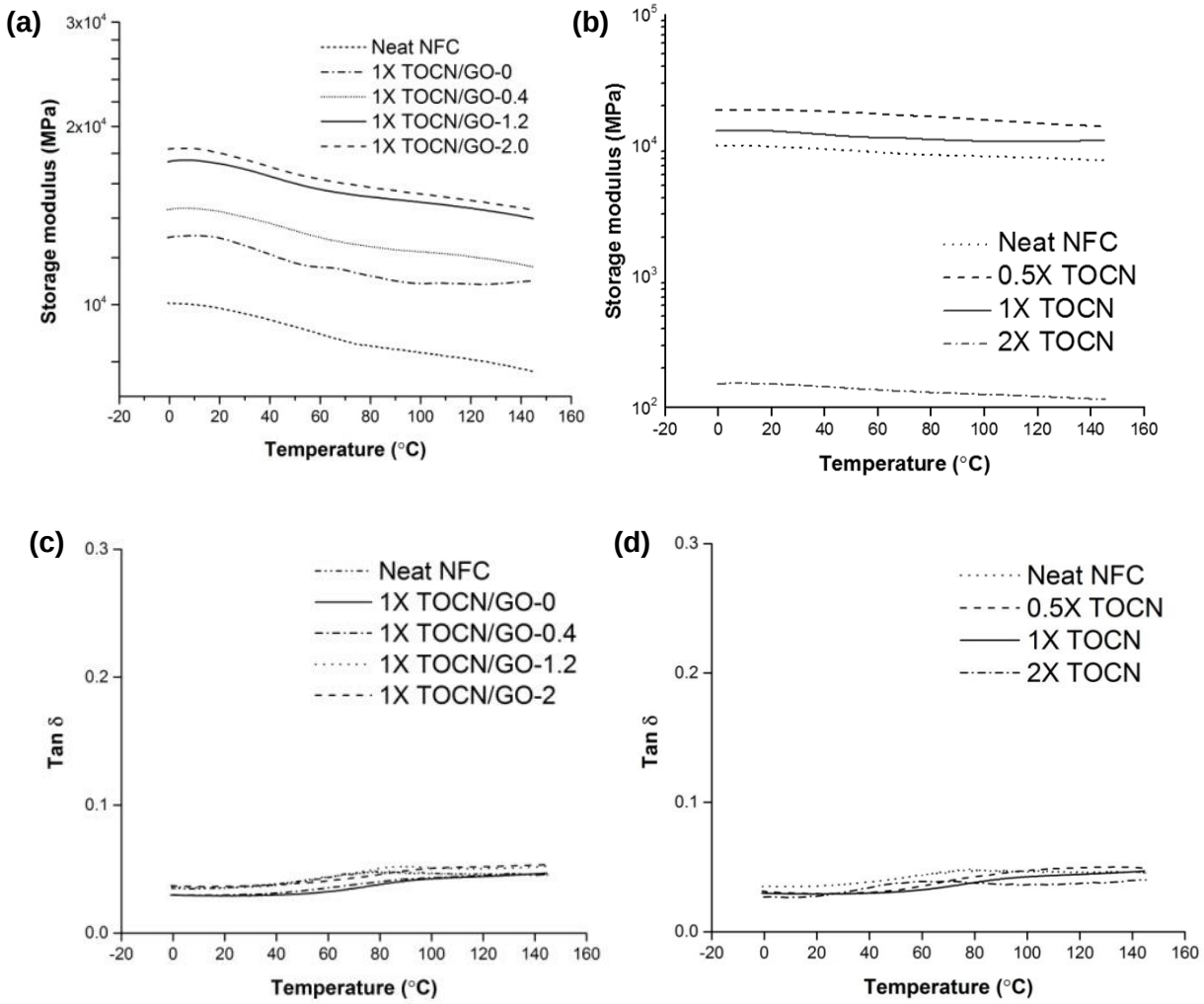

Figure 3. Storage moduli of the TOCN/GO composite samples with different content of graphene oxide (GO) (a) and different degree of oxidation (b). Tan δ of the TOCN films with different content of graphene oxide (GO) (C) and different degree of oxidation (d)

1X TOCN/GO-2 showed the highest storage modulus over the whole temperature range. The enhancement of storage modulus is caused by the effective load transfer from TEMPO-oxidized cellulose matrix to GO nanofillers. The storage modulus of TOCN/GO nanocomposites

with loadings of 0, 0.4, 1.2, and 2% at 23 °C correspond to %-increases of 13%, 25%, 51%, and 57%, respectively, compared to neat NFC. As for the effect of the degree of oxidation, the TEMPO oxidation caused an increase in storage modulus in accordance with the results obtained from Johnson et al.[6]The increase of storage modulus with the increasing oxidation level can be explained by stronger fibrous network and entanglements of highly separated fibril, limiting the segmental backbone motion of the cellulose chains around the nanofillers.[22,23] The dynamic moduli of 0.5X and 1X TOCN films, comparing to neat NFC, created a stronger TOCN structure when there is an optimal concentration of TEMPO and NaBr for oxidation. The storage modulus of 1X TOCN was increased by 12% compared to neat NFC. However, the most extremely oxidized cellulose was different from what was expected, the better interaction upon more disintegration. A 2X TOCN film represented an approximately 100-fold decrease in storage modulus at 23 °C due to the increased void volume by severe oxidation. Despite the large number of interconnected network between fibrils as predicted, the void volume generated on the surface was dominated in this case.

Tan δ (E"/E'), also called a damping factor, indicates the dissipated energy of a polymer.[21]However, peak broadening of TOCN/GO nanocomposites and shift of the tan δ peaks were not detected as shown in Figure 3.The change in tan δ of TOCN on heating is not significant as reported by Bulota et al.[21]

3.5.5. Mechanical properties

The improvement in the mechanical property of the nanocomposites is determined by the dispersion state, the degree of exfoliation of GO, and interfacial interaction between polymer matrix and nanofillers. Wang et al. found that the tensile strength of regenerated MCC

(microcrystalline cellulose) composite films with addition of 0.5 wt% of GO increased by 64.7%.[8] However, the mechanical properties of regenerated MCC-GO composites were lower than that of neat MCC film with the GO content over 1 wt% due to inhomogeneous dispersion of GO in the polymer matrix. The average values of tensile strength are shown in Figure 4(a). In addition, the Young's moduli increased from 1.1 GPa for neat NFC to 1.3, 1.5, 1.6 and 2.1 GPa for TOCN/GO-0, 0.4, 1.2, and 2.0, respectively. Based on our study, the tensile strength of TOCN films consistently increase as the % loadings of GO increase except for the 2 wt% GO addition (107 MPa). The decreased mechanical performance of TOCN/GO-2 can be explained by the decreased intermolecular cohesiveness between polymer matrix and reinforcing phases since it went beyond the greatest load, causing the aggregation.

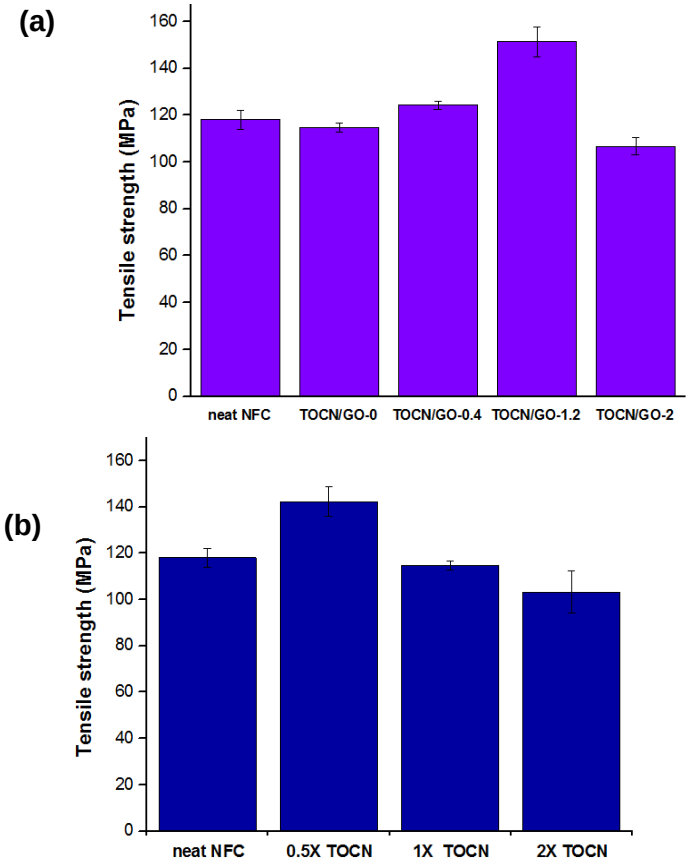

Figure 4. Tensile strength of neat NFC and TOCN/GO composite films with different content of graphene oxide (GO) (a) and different degree of oxidation (b)

Table2. Statistical evaluation with the Tukey Method

Effect of graphene oxide content		Effect of degree of oxidation	
Sample	**Grouping**	**sample**	**Grouping**
neat NFC	B	neat NFC	A B
1X TOCN/GO-0	B	0.5X TOCN	A
1X TOCN/GO-0.4	B	1X TOCN	A B
1X TOCN/GO-1.2	A	2X TOCN	B
1X TOCN/GO-2	B		

Sampleswhich do not have the same letter are significantly different

Han and Feng et al. reported that the regenerated cellulose composite films with high concentration of GO improved the tensile strength by forming hydrogen bonds;[24-25] on the contrary, the composite films with high loadings of GO studied by Zhang et al. showed a reduction in mechanical property when it went beyond a critical loading, which was caused by poor distribution state and the restacking of graphene oxide layers.[26]

Figure 4(b) represents the different tensile strength tendencies upon the degree of oxidation. The tensile strength of 0.5X TOCN film is superior to that of other films, and they tend to decrease as the oxidation level increases. As analyzed by the DMA, 2X TOCN indicates a drastic reduction in mechanical property since the increased number of hydrogen bonds between TOCNs and GO was not enough to offset the void volume. This result is also correlated to the SEM analysis.

3.5.6. Morphology of TOCN/GO nanocomposite films

A FE-SEM (field emission scanning electron microscopy) was used to investigate the uniformity of fibril layers and any morphological changes upon the different degree of oxidation and GO loadings. According to the several studies, it has been found that the surface modification via TEMPO does not have an influence on the morphology of any TOCN samples.[5] Even with the introduction of the high amount of carboxylate groups, the original cellulose

structure tends to be sustained since the oxidation preferably occurs on the surfaces and amorphous disordered regions.[18] However, other studies reported some morphological changes after oxidation. The commonly observed layered structure of randomly assembled fibers can result from the disintegrated fibril interactions, followed by the formation of hydrogen bonds among adjacent fibrils in a parallel direction, creating a layer structure. The layers are piled up on another layer via interlayer van der Waals forces in the a-b plane of the unit cell, which is perpendicular to the chain axis.[27-28]

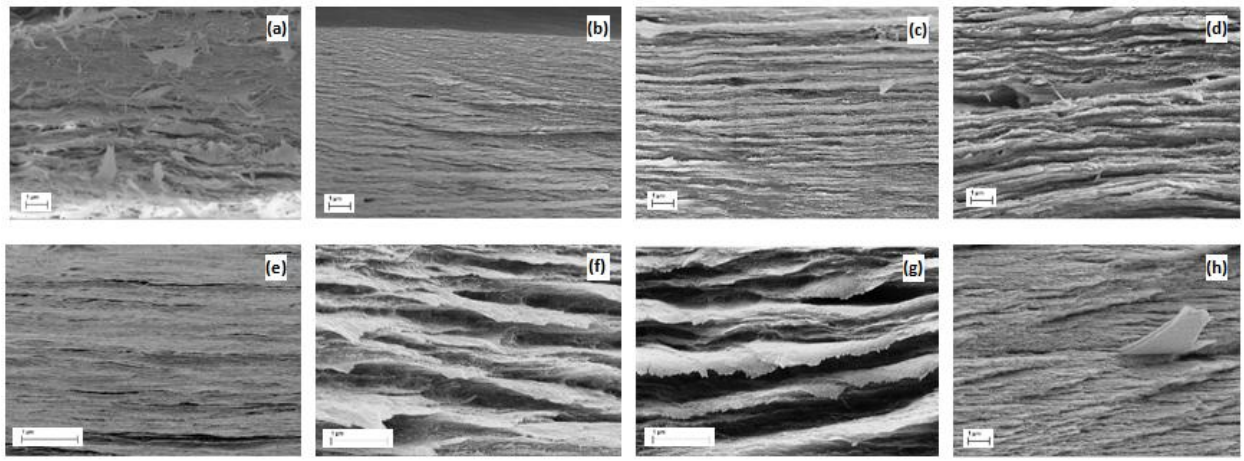

Figure 5. The cross-sectional SEM images of neat NFC (a), 0.5X TOCN (b), 1X TOCN/GO-0 (c), 2X TOCN (d), 1X TOCN/GO-0.4 (e), 1X TOCN/GO-1.2 (f), 1X TOCN/GO-2 (g), and the protruded graphene oxide sheets (h)

The SEM images of neat NFC still demonstrate randomly oriented fibril bundles in a less compact form. In contrast, cross-sectional SEM images of TOCN nanocomposite films revealed considerably fibrous and dense layered structure, composed of thin individual fibril layers. In our study, all TOCN films display highly interconnected and compact cellulose layers in comparison with neat NFC, but 2X TOCN has relatively larger and less dense layers, along with an increased void volume, caused by the extreme oxidation.[29]

Furthermore, with the incorporation of GO, the TOCN/GO films show the homogeneity from the interior to the surface, which might lead to a good adhesion between nanofillers and the polymer matrix. As a result, GO sheets can increase the reinforcement ability in the nanocomposites and successfully transfer the load from the TOCN matrix to GO unless it goes beyond the critical loading. Meanwhile, since the well-exfoliated GO layers were intercalated into the TOCN matrix rather than stacked on the top of each other, they were rarely found in the SEM images as presented in Figure 5. Han et al. reported that the apparent grooves created by fracturing the films were ascribed to uneven stiffness and composite network between TOCN and GO.[30] In our work, as the contents of GO increase, especially in 1X TOCN/GO-2, more obvious stratification phenomenon can be observed.

3.5.7. Gas permeation properties of neat NFC and TOCN/GO nanocomposites

Water vapor and oxygen barrier properties play significant roles in food packaging since food decay is vulnerable to these two factors. Water vapor transmission rate (WVTR) is measured by the amount of water vapor passing through the film per time and unit area until it reaches steady state. There are several physico-chemical parameters influencing the WVTR of films such as chemical composition, orientation, polarity, crystallinity and void volume. Typically, the higher degree of the crystallinity impedes the diffusion of water vapor molecules through the impermeable crystalline regions due to more organized and dense network.[31] However, there was no significant difference in crystallinity as observed in XRD, so the change in barrier permeability can be explained by other factors, such as the void volume, tortuous pathways, and a strong fibrous network formed by intermolecular interactions between the oxidized cellulose and nanofillers. A series of water and gas permeation tests on TOCN/GO

nanocomposites were carried out, and the results are presented in Table 3,4. Since the thickness of the film is one of the parameters affecting the transmission rate by limiting the diffusion of oxygen and water molecules through the films,[32] the OTR and WVTR values were normalized.

Table 3. Water vapor permeability of neat NFC and TOCN/GO nanocomposite films

Effect of graphene oxide content		Effect of degree of oxidation	
sample	**WVP**	**Sample**	**WVP**
neat NFC	3.780 (±0.21)	neat NFC	3.780 (±0.21)
1X TOCN/GO-0	0.838 (±0.11)	0.5X TOCN	1.094 (±0.22)
1X TOCN/GO-0.4	0.795 (±0.21)	1X TOCN	0.838 (±0.11)
1X TOCN/GO-1.2	1.650 (±1.24)	2X TOCN	3.288 (±0.90)
1X TOCN/GO-2	1.140 (±0.20)		
Unit of permeability coefficient (P): g·cm/cm2·s·Pa (P X 10^{-13})			

The cellulosic materials tend to show higher values in the WVP compared to one of the conventionally used packaging materials, low density polyethylene (LDPE) ($9.14X10^{-15}$ g·cm/cm^2·s·Pa).[33] Their WVPs remained higher because the hydrophilic cellulosic materials have a higher water affinity of their surfaces; additionally, the severe oxidation led to the cellulosic network structure more loosened by the negative electrostatic repulsion.[32]

As shown in Table 3, all the WVPs among the different concentrations of GO were not significantly different from each other. However, the WVPs decreased after the moderate TEMPO-mediated oxidation, such as 0.5X and 1X TOCN, and increased again at 2X TOCN. This might result from an increased surface nanoporosity from the remarkably liberated fibrils when the extreme oxidation with the highest concentration of catalysts was applied.

Although the water vapor barrier properties were still insufficient overall due to the hygroscopic nature of NFC, cellulosic materials generally tend to exhibit good oxygen barrier properties since the polar polysaccharides hinder the permeation of non-polar oxygen molecules by the repulsion.

Table 4. OTR values of neat NFC and TOCN/GO nanocomposites at different loadings (a) and different degree of oxidation (b)

Effect of graphene oxide content		Effect of degree of oxidation	
Sample	**OTR**	**sample**	**OTR**
neat NFC	993.3 (±81.1)	neat NFC	993.3 (±81.1)
1X TOCN/GO-0	669.7 (±37.3)	0.5X TOCN	176.2 (±9.7)
1X TOCN/GO-0.4	239.8 (±4.3)	1X TOCN	669.7 (±37.3)
1X TOCN/GO-1.2	175.4 (±34.9)	2X TOCN	Not measurable
1X TOCN/GO-2	353.3 (±26.3)		

Unit of oxygen transmission rate: $g/m^2/day$

All OTR values of TOCN films measured at 0% RH are higher than that of neat NFC. The TEMPO oxidation formed a highly packed cellulose network generated by fibrils with smaller dimensions as observed in the SEM images. With respect to the effect of GO, the incorporated GO sheets enhanced the barrier properties by forming tortuous pathways against the oxygen molecules and retarding the diffusion of permeable gas molecules through the TOCN matrix. Meanwhile, the transmission rate of non-polar oxygen molecules might be influenced by polarity of the film, expecting the increase in OTR since the C/O ratio in NFC is roughly 1.2, and the C/O ratio of GO is close to 2. However, the effect of the increased tortuosity and intermolecular interaction between the negatively charged TOCNs and GO were greater than that of the slight reduction in polarity after the addition of GO, resulting in the decrease in OTR values. In this study, the oxygen permeability of the TOCN film with 1.2% GO showed the lowest value as 175ml/m²/day, which was even lower than that of 2% GO added film. Therefore, the 1.2% GO addition to the cellulose matrix is determined to be an optimal concentration in improving the barrier properties. As for the effect of the degree of oxidation, the higher oxidation level (1X TOCN) compared to 0.5X TOCN induced a decrease in the OTR from 669 ml/m²/day to 176 ml/m²/day. As the OTR of 2X TOCN was expected to show the highest OTR value, but the consistent oxygen gas flow over time was not measurable. The reduced entanglement with

shorter lengths of fibrils may have an influence on OTRs of the TOCN films since the severe oxidation treatment tend to lower the degrees of polymerization of TOCN fibrils. Therefore, its exceptionally increased surface area, that is, void volume, occurred as results of the less entanglement of the fibrils. It is concluded that the WVPs are still high, whereas the oxygen barrier properties were enhanced after the treatments.

3.5.8. Effect of TEMPO oxidation on thermal properties of the nanocomposites

Figure 6 presents the onset temperature of thermal degradation of TOCN-GO nanocomposites with different GO loadings. The TGA profiles of TOCN-GO nanocomposites exhibit three remarkable weight loss transitions. The first zone below 100 °C is attributed to the loss of moisture.[14] The major weight loss observed in the range of 217-338 °C is due to the release of the oxygen-containing functional groups of thermally unstable graphene oxide, such as hydroxyl and epoxy, and decarboxylation of TOCNs.[14, 34] The last degradation region, above ~480 °C, is assigned to the degradation of graphene oxide in the composites.

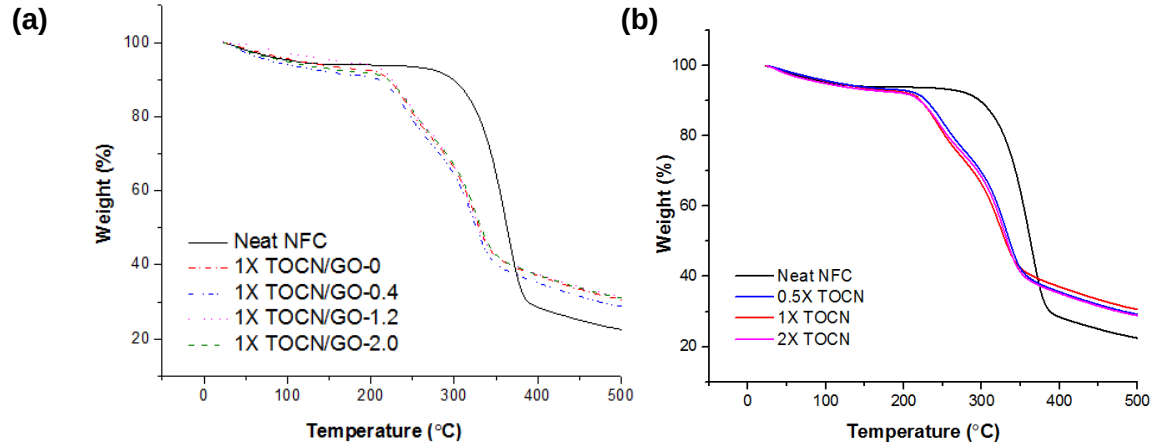

Figure 6. TGA curves for neat NFC and TOCN/GO composites at different GO loadings (a) and degree of oxidation (b)

All TOCN films after the oxidation represent a distinctive effect on thermal degradation temperature. The TEMPO treatment was effective in promoting the thermal degradation owing to decarboxylation of anhydroglucuronate units via carbanion formation upon heating.[35]Fukuzumi et al. also reported that the onset of thermal degradation of NFC with surface modification via TEMPO-mediated oxidation shifted to a lower temperature region.[36] Pristine NFC was about 100 °C higher than that of TEMPO treated NFC.[37] It corresponds to our TGA results. As for TEMPO treated 1X TOCN/GO-0, the thermal degradation rate was noticeably increased compared to the original NFC in Figure 6. The degradation temperature of the oxygen-containing functional groups decreased by 100°C. It could be explained that the larger surface area accompanied by the chemical and mechanical disintegration processes promoted the more exposed portions of cellulose, leading to higher weight loss per unit rise in temperature.[32] However, the TGA curves for TOCNs with carboxylate groups of 0.280, 0.370, 0.425 mmol/g were undistinguishable, and the addition of GO does not highly affect the thermal degradation of the TOCN nanocomposites.

3.6. Conclusions

The TOCN/GO composite films were prepared by incorporation of GO and TEMPO-oxidation to investigate the effects of GO nanofillers and oxidation levels. When the amounts of TEMPO and NaBr were increased, the corresponding carboxylate group content was also increased. The well-exfoliated GO nanofillers with various GO content in the TOCN matrix were verified by XRD. FTIR spectra display the increased density of carboxylate groups as the GO content and degree of oxidation increase. Cross-sectional SEM micrographs of TOCN/GO composites represented the morphological changes. For example, it showed thicker and less

dense layered structures upon the TEMPO-catalyzed reaction and inclusion of nanofillers, compared to neat NFC. Nevertheless, TOCN composites at 1.2% and 2% GO loadings exhibited the obvious improvement in tensile strength and storage modulus due to the strong intermolecular cohesiveness between GO sheets and the cellulose matrix. On the contrary, as for 2X TOCN, the increased void volume, caused by intense fibrillation on surfaces, induced a remarkable decrease in both storage modulus and tensile strength. It corresponds to the results of gas and water vapor permeation properties. The highest oxidation level allowed for a significant increase in the OTR and WVP. In terms of the effect of the various GO content, the OTR value of 1X TOCN/GO-1.2 was decreased by 82% compared to neat NFC, whereas the WVPs of TOCN/GO composites at different GO loadings were almost identical. The TGA analysis of thermal properties of neat NFC and TOCN/GO nanocomposites resulted in a promoted thermal degradation of TOCN films owing to an increase of the exposed surface area.

REFERENCES

1. Mohanty, A.; Misra, M.; Drzal, L., Sustainable bio-composites from renewable resources: opportunities and challenges in the green materials world. *Journal of Polymers and the Environment* **2002,***10* (1), 19-26.
2. Koga, H.; Saito, T.; Kitaoka, T.; Nogi, M.; Suganuma, K.; Isogai, A., Transparent, conductive, and printable composites consisting of TEMPO-oxidized nanocellulose and carbon nanotube. *Biomacromolecules* **2013,***14* (4), 1160-1165.
3. Herrick, F. W.; Casebier, R. L.; Hamilton, J. K.; Sandberg, K. R. In *Microfibrillated cellulose: morphology and accessibility*, J. Appl. Polym. Sci.: Appl. Polym. Symp.;(United States), ITT Rayonier Inc., Shelton, WA: 1983.
4. Saito, T.; Kimura, S.; Nishiyama, Y.; Isogai, A., Cellulose nanofibers prepared by TEMPO-mediated oxidation of native cellulose. *Biomacromolecules* **2007,***8* (8), 2485-2491.
5. Saito, T.; Nishiyama, Y.; Putaux, J.-L.; Vignon, M.; Isogai, A., Homogeneous suspensions of individualized microfibrils from TEMPO-catalyzed oxidation of native cellulose. *Biomacromolecules* **2006,***7* (6), 1687-1691.
6. Johnson, R. K.; Zink-Sharp, A.; Renneckar, S. H.; Glasser, W. G., A new bio-based nanocomposite: fibrillated TEMPO-oxidized celluloses in hydroxypropylcellulose matrix. *Cellulose* **2009,***16* (2), 227-238.
7. Wan, C.; Chen, B., Reinforcement of biodegradable poly (butylene succinate) with low loadings of graphene oxide. *Journal of Applied Polymer Science* **2013,***127* (6), 5094-5099.
8. Wang, B.; Lou, W.; Wang, X.; Hao, J., Relationship between dispersion state and reinforcement effect of graphene oxide in microcrystalline cellulose–graphene oxide composite films. *Journal of Materials Chemistry* **2012,***22* (25), 12859-12866.
9. Yao, X.; Yu, W.; Xu, X.; Chen, F.; Fu, Q., Amphiphilic, ultralight, and multifunctional graphene/nanofibrillated cellulose aerogel achieved by cation-induced gelation and chemical reduction. *Nanoscale* **2015,***7* (9), 3959-3964.
10. Wei, H.; Rodriguez, K.; Renneckar, S.; Vikesland, P. J., Environmental science and engineering applications of nanocellulose-based nanocomposites. *Environmental Science: Nano* **2014,***1* (4), 302-316.
11. Hummers Jr, W. S.; Offeman, R. E., Preparation of graphitic oxide. *Journal of the American Chemical Society* **1958,***80* (6), 1339-1339.
12. Jiang, F.; Han, S.; Hsieh, Y.-L., Controlled defibrillation of rice straw cellulose and self-assembly of cellulose nanofibrils into highly crystalline fibrous materials. *Rsc Advances* **2013,***3* (30), 12366-12375.
13. Coates, J., Interpretation of infrared spectra, a practical approach. *Encyclopedia of analytical chemistry* **2000**.
14. Mandal, B.; Das, D.; Rameshbabu, A. P.; Dhara, S.; Pal, S., A biodegradable, biocompatible transdermal device derived from carboxymethyl cellulose and multi-walled carbon nanotubes for sustained release of diclofenac sodium. *RSC Advances* **2016,***6* (23), 19605-19611.
15. Liu, D.; Bian, Q.; Li, Y.; Wang, Y.; Xiang, A.; Tian, H., Effect of oxidation degrees of graphene oxide on the structure and properties of poly (vinyl alcohol) composite films. *Composites Science and Technology* **2016,***129*, 146-152.

16. Chen, Y.; Xie, B.; Ren, Y.; Yu, M.; Qu, Y.; Xie, T.; Zhang, Y.; Wu, Y., Designed nitrogen doping of few-layer graphene functionalized by selective oxygenic groups. *Nanoscale research letters* **2014,***9* (1), 646.
17. Shao, W.; Liu, H.; Liu, X.; Wang, S.; Zhang, R., Anti-bacterial performances and biocompatibility of bacterial cellulose/graphene oxide composites. *RSC Advances* **2015,***5* (7), 4795-4803.
18. Saito, T.; Okita, Y.; Nge, T.; Sugiyama, J.; Isogai, A., TEMPO-mediated oxidation of native cellulose: Microscopic analysis of fibrous fractions in the oxidized products. *Carbohydrate polymers* **2006,***65* (4), 435-440.
19. Siró, I.; Plackett, D., Microfibrillated cellulose and new nanocomposite materials: a review. *Cellulose* **2010,***17* (3), 459-494.
20. Zhang, C.; Zhu, X.; Wang, Z.; Sun, P.; Ren, Y.; Zhu, J.; Zhu, J.; Xiao, D., Facile synthesis and strongly microstructure-dependent electrochemical properties of graphene/manganese dioxide composites for supercapacitors. *Nanoscale research letters* **2014,***9* (1), 490.
21. Bulota, M.; Vesterinen, A. H.; Hughes, M.; Seppälä, J., Mechanical behavior, structure, and reinforcement processes of TEMPO-oxidized cellulose reinforced poly (lactic) acid. *Polymer Composites* **2013,***34* (2), 173-179.
22. Srithep, Y.; Turng, L.-S.; Sabo, R.; Clemons, C., Nanofibrillated cellulose (NFC) reinforced polyvinyl alcohol (PVOH) nanocomposites: properties, solubility of carbon dioxide, and foaming. *Cellulose* **2012,***19* (4), 1209-1223.
23. Bettaieb, F.; Nechyporchuk, O.; Khiari, R.; Mhenni, M. F.; Dufresne, A.; Belgacem, M. N., Effect of the oxidation treatment on the production of cellulose nanofiber suspensions from Posidonia oceanica: The rheological aspect. *Carbohydrate polymers* **2015,***134*, 664-672.
24. Feng, Y.; Zhang, X.; Shen, Y.; Yoshino, K.; Feng, W., A mechanically strong, flexible and conductive film based on bacterial cellulose/graphene nanocomposite. *Carbohydrate Polymers* **2012,***87* (1), 644-649.
25. Han, D.; Yan, L.; Chen, W.; Li, W.; Bangal, P., Cellulose/graphite oxide composite films with improved mechanical properties over a wide range of temperature. *Carbohydrate Polymers* **2011,***83* (2), 966-972.
26. Zhang, H.; Wang, Z.; Zhang, Z.; Wu, J.; Zhang, J.; He, J., Regenerated-Cellulose/Multiwalled-Carbon-Nanotube Composite Fibers with Enhanced Mechanical Properties Prepared with the Ionic Liquid 1-Allyl-3-methylimidazolium Chloride. *Advanced Materials* **2007,***19* (5), 698-704.
27. Lai, C.; Sheng, L.; Liao, S.; Xi, T.; Zhang, Z., Surface characterization of TEMPO-oxidized bacterial cellulose. *Surface and Interface Analysis* **2013,***45* (11-12), 1673-1679.
28. Cousins, S. K.; Brown Jr, R. M., X-ray diffraction and ultrastructural analyses of dye-altered celluloses support van der Waals forces as the initial step in cellulose crystallization. *Polymer* **1997,***38* (4), 897-902.
29. Luo, H.; Xiong, G.; Hu, D.; Ren, K.; Yao, F.; Zhu, Y.; Gao, C.; Wan, Y., Characterization of TEMPO-oxidized bacterial cellulose scaffolds for tissue engineering applications. *Materials Chemistry and Physics* **2013,***143* (1), 373-379.
30. Han, D.; Yan, L.; Chen, W.; Li, W., Preparation of chitosan/graphene oxide composite film with enhanced mechanical strength in the wet state. *Carbohydrate Polymers* **2011,***83* (2), 653-658.

31. Syverud, K.; Stenius, P., Strength and barrier properties of MFC films. *Cellulose* **2009,***16* (1), 75.
32. Lavoine, N.; Desloges, I.; Dufresne, A.; Bras, J., Microfibrillated cellulose–Its barrier properties and applications in cellulosic materials: A review. *Carbohydrate polymers* **2012,***90* (2), 735-764.
33. Gutiérrez-López, G. F.; Welti-Chanes, J.; Parada-Arias, E., *Food engineering: Integrated approaches*. Springer Science & Business Media: 2008.
34. Wang, X.; Hu, Y.; Song, L.; Yang, H.; Xing, W.; Lu, H., In situ polymerization of graphene nanosheets and polyurethane with enhanced mechanical and thermal properties. *Journal of materials Chemistry* **2011,***21* (12), 4222-4227.
35. Fukuzumi, H.; Saito, T.; Okita, Y.; Isogai, A., Thermal stabilization of TEMPO-oxidized cellulose. *Polymer Degradation and Stability* **2010,***95* (9), 1502-1508.
36. Fukuzumi, H.; Saito, T.; Iwata, T.; Kumamoto, Y.; Isogai, A., Transparent and high gas barrier films of cellulose nanofibers prepared by TEMPO-mediated oxidation. *Biomacromolecules* **2008,***10* (1), 162-165.
37. Moon, R. J.; Martini, A.; Nairn, J.; Simonsen, J.; Youngblood, J., Cellulose nanomaterials review: structure, properties and nanocomposites. *Chemical Society Reviews* **2011,***40* (7), 3941-3994.